HHS Public Access

Author manuscript

ACS Chem Biol. Author manuscript; available in PMC 2020 August 16.

Published in final edited form as:

ACS Chem Biol. 2019 August 16; 14(8): 1687–1692. doi:10.1021/acschembio.9b00263.

The global repair profile of human alkyladenine DNA glycosylase on nucleosomes reveals DNA packaging effects

Erin E. Kennedy[a], **Chuxuan Li**[b], **Sarah Delaney**[a,b,*]

[a]Department of Molecular Biology, Cell Biology, and Biochemistry, Brown University, Providence, RI 02912, United States

[b]Department of Chemistry, Brown University, Providence, Rhode Island 02912, United States

Abstract

Alkyladenine DNA glycosylase (AAG) is the only known human glycosylase capable of excising alkylated purines from DNA, including the highly mutagenic 1,N^6-ethenoadenine (εA) lesion. Here we examine AAG's ability to excise εA from a nucleosome core particle (NCP), which is the primary repeating unit of DNA packaging in eukaryotes. Using chemical synthesis techniques, we assembled a global population of NCPs in which A is replaced with εA. While each NCP contains no more than one εA lesion, the total population contains εA in 49 distinct geometric positions. Using this global εA-containing NCP system, we obtained kinetic parameters of AAG throughout the NCP architecture. We observed monophasic reaction kinetics across the NCP, but varying amounts of AAG excision. AAG activity is correlated with solution accessibility and local histone architecture. Notably, we identified some highly solution-accessible lesions that are not repaired well, and an increase in repair within the region of asymmetric unwrapping of the nucleosomal DNA end. These observations support *in vivo* work and provide molecular-level insight into the relationship between repair and NCP architecture.

Graphical Abstract

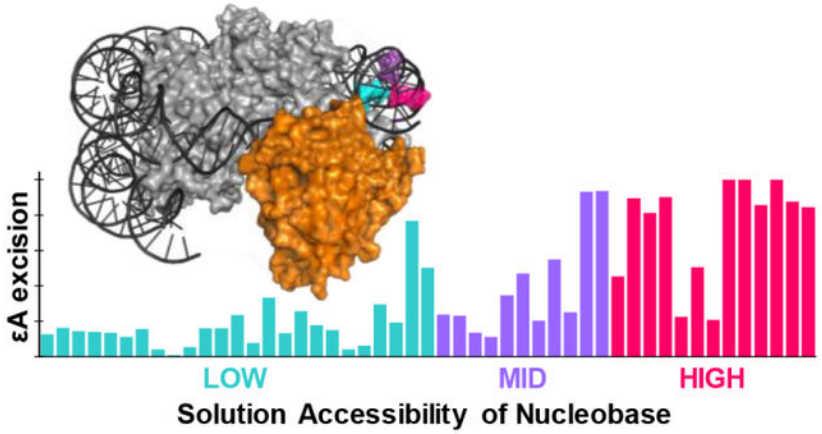

* sarah_delaney@brown.edu.

Supporting Information Available: This material is available free of charge via the Internet. DNA sequences and ligation schemes, supplementary figures and tables (including gel images, k_{obs} values, and DNase I footprinting), and detailed materials and methods.

Despite its being the code of life, DNA has a physiochemical composition that makes it susceptible to modification and decomposition by endogenous and exogenous sources.[1] Failure to rectify these modifications can result in mutagenic consequences such as cancer.[2] The repair of nucleobase lesions can be accomplished with the base excision repair (BER) pathway. BER is initiated by a glycosylase enzyme specialized for removing a particular lesion(s).[3] Most glycosylases use a base-flipping mechanism to extrude the lesion from the helix and catalyze *N*-glycosidic bond cleavage, resulting in an abasic site.[4] Interestingly, alkyladenine DNA glycosylase (AAG) is the only known human glycosylase that removes alkylated nucleobases, including 3-methyladenine, 7-methylguanine, and 1,N^6-ethenoadenine (εA).[5] Specifically, εA can be generated by environmental exposure to vinyl chloride, or by attack of endogenous lipid peroxidation products (Figure 1A).[6] The current study focuses on the removal of εA by AAG.

Many prior studies characterized glycosylase activity using short oligonucleotide duplex substrates. However, eukaryotic DNA is highly packaged, presenting a more complicated environment for repair *in vivo*. The primary repeating unit of chromatin is the nucleosome core particle (NCP) (Figure 1B) with 75–90% of genomic DNA packaged as such.[7] NCPs consist of 145–147 bp of DNA wrapped in ~1.7 left-handed superhelical turns around an octameric core of histone proteins.[8] The histone core contains two copies of each histone, H2A, H2B, H3, and H4, with two-fold rotational symmetry about a dyad axis. As a consequence of wrapping around the histone core, the DNA becomes structurally distorted and locally stretched.[9] The presence of the histones also means that there are regions of DNA that are sterically blocked while other regions are physically more accessible to DNA-binding proteins.[10]

The geometric position of a nucleobase in an NCP can be described in two ways: the rotational position and the translational position. Rotational positioning of a nucleobase refers to its helical orientation; i.e. if the lesion is facing outward toward solution, or inward toward the histone core. Translational positioning refers to the location of the nucleobase relative to the dyad axis. It has been shown that nucleobases located toward the ends of the DNA have increased solution accessibility compared with those near the dyad region due to transient and spontaneous DNA unwrapping.[10,11]

Previous studies have shown that geometric positioning of a lesion and local histone environment can modulate glycosylase activity on an NCP.[12] Most of these previous studies created NCPs containing a site-specific lesion. To obtain information about activity in other NCP regions, additional site-specific lesion-containing NCPs were created with the lesion in a different geometric position. These initial experiments showed that each local histone environment had varying effects on glycosylase activity beyond solution accessibility. Because every nucleobase in an NCP inherently has a unique microenvironment, no lesion location can be used as a representative of repair in a packaged DNA context. Furthermore, although studies using site-specific lesions in NCPs are informative, it would be time-consuming and impractical to study DNA repair across the entirety of the nuanced NCP architecture containing 145–147 bp in this manner.

With these considerations in mind, we recently designed a global system for simultaneous study of multiple lesion positions, and therefore probing of multiple NCP microenvironments, to describe glycosylase activity across an NCP.[13] Global lesion-containing DNA is prepared by chemical synthesis using a building block mixture of the lesion of interest and the unmodified nucleobase that maximizes the number of strands containing 0 or 1 lesion throughout the sequence. Reconstitution of NCPs using global lesion-containing duplex and histone octamer yields a population of NCPs with the lesion positioned in a variety of well-defined translational and rotational positions. Here, we utilize the global system to substitute εA for A in either the I or J strand of the Widom 601 NCP[14] to study excision by AAG in a total of 49 distinct geometric positions (Figure 1C, Scheme S1, Figure S1). Whereas our previous work qualitatively described repair of 8-oxo-7,8-dihydroguanine lesions in NCPs, our current work elevates the global system to provide kinetic parameters to describe εA excision by AAG in duplex controls and NCPs.

We first measured εA excision by AAG as a function of time in a 145 bp global duplex control (DUP) (Figure 2A and Figure S2A). DUP was assembled with one εA-containing 145 mer annealed to the undamaged complementary strand (Scheme S2). Due to the small amount of each lesion-containing substrate relative to the total DNA population, we defined the amount of excised product observed after 180 min as the maximal product accumulation at a given lesion site. We chose an 180 min time course based on previous experiments and AAG's slow activity,[5,15] and confirmed that AAG retains full activity over the 180 min (Figure S3). Therefore, product accumulation at time t is represented as a ratio relative to product accumulation at 180 min (DUP_t/DUP_{180}) (Figure S4). Monophasic fits of reaction progress at each lesion site in DUP (Figure 2B, closed symbols) determined the observed rate (k_{obs}) of AAG excision at the 49 εA positions in DUP, which ranges from 0.030–0.091 min^{-1} (Table S1). These k_{obs} values are comparable to previous reports for site-specific εA lesions in both short oligonucleotide duplexes[5,15] and 145 bp duplex.[16]

We next prepared global εA-containing NCP populations to examine AAG activity in packaged DNA (Figure S5). We previously reported[13,16,17] extensive control experiments to determine strategies that minimize, to the greatest extent possible, unincorporated DNA in NCP preparations. Only NCP preparations with ≤5% DUP are used in experiments. Product accumulation in the NCP was determined at time t as a ratio relative to maximal product accumulation, NCP_t/DUP_{180} (Figure 2A,C; Figure S2). Unlike AAG excision from DUP, not all εA lesions in NCPs were fully excised by 180 min; 30/49 sites had less than 30% excision (Figure S6). Suppressed activity relative to DUP indicates that the presence of the histone octamer interferes with AAG activity. We verified that all DNA containing εA lesions formed NCPs and there was no bias in NCP formation based on the geometric position of the lesion (Figure S7); therefore, a lack of excision from NCPs is due to a lack of AAG activity.

We next obtained k_{obs} describing AAG excision of εA from the global NCPs. As observed for DUP, excision of εA across NCPs displayed monophasic behavior (Figure 2B, open symbol). In addition, k_{obs} values across NCPs are comparable to those observed in DUP and to those obtained for a site-specific lesion in an NCP (Table S1).[16] However, different from results observed with DUP, significantly suppressed excision efficiency is observed at 30/49

sites. The monophasic behavior of AAG in DUP and NCP, paired with the varying amounts of εA excision in NCPs, suggests that there are subpopulations of NCPs that are conformationally competent for AAG activity while others are not. The NCP population that is unrepaired by AAG is not due to the DNA substrates being chemically incompetent. Instead, the population is not repaired due to a structural impediment and/or conformation derived from the histone octamer which renders the lesion inaccessible to AAG activity. In the cell, repair of these lesions might require chromatin remodelers and/or additional factors. Previous kinetic characterizations of human glycosylases OGG1 and UNG2 acting on site-specific lesion NCP systems revealed multiphasic kinetics (≥2 phases) for removal of lesions in some positions, which was attributed to conformation changes in the NCP.[17,18] Considering AAG's slower rate of glycosylase activity compared with OGG1 and UNG2, the monophasic behavior observed across the NCP suggests that analogous conformational changes cannot be resolved on this timescale.

Next, we evaluated the relationship between AAG activity and solution accessibility of each εA lesion. We performed hydroxyl radical footprinting (HRF) to characterize solution accessibility of nucleobases in global NCPs (Figure 3, shaded gray area; Figure S8). εA positions with high (HIGH), medium (MID), and low (LOW) solution accessibilities were grouped based on the ratios of accessibility to the maximal accessibility within a helical turn of the HRF profile (Table S2). Overall, we found the extent of εA excision from NCPs by AAG is highly correlated with solution accessibility, similar to our previous observations of the global repair profiles of OGG1[13] and UDG[19] on NCPs. About half of the HIGH positions, i.e. sites 42, 64, −103, −104, 105, −114, had maximal εA excision (90–100%). Conversely, minimal amounts of product were observed at most LOW positions, with no greater than 20% εA excision. MID positions had low to moderate εA excision, ranging from 10–60%. The broader range of εA excision observed at MID positions is likely due to varied NCP microenvironments. For example, MID positions with less than 20% εA excision are located near histone tails; sites −34, −37, −47, −111 are closest to the base of an H2A tail, and position 119 is similarly near an H2B tail. Indeed, other glycosylases[17,20] and BER enzymes[21] have shown variable amounts of inhibition due to histone tails. The proximity of histone tails to certain positions may interfere with AAG in similar ways to reduce activity.

We also used DNase I footprinting as a complementary approach to HRF to characterize the solution accessibility of nucleobases using an enzymatic probe of similar size to that of AAG (molecular weight of DNase I is 29 kDa versus 26 kDa for AAG) (Figure S9, S10). The local maxima of accessibility within a helical turn are consistent with those observed by HRF (Figure S11).

The overall correlation between glycosylase activity and solution accessibility observed in these *in vitro* chromatin experiments is consistent with *in vivo* observations. A study in yeast mapped alkylation damage and its subsequent repair by the yeast homolog of AAG across the genome;[22] the examination of 10,000 strongly-positioned NCPs in the genome revealed decreased repair at less solution-accessible sites. Another recent study reported that somatic mutational rates in ~3,500 human tumors are enriched in sequences packaged by NCPs.[23] Further, a subset of tumor types had a relative increase in mutation rates where minor

grooves faced the histone core, specifically attributed to decreased repair at less-accessible positions.

A reduction of AAG activity within chromatin may lead to this imbalance in DNA damage and repair that could cause mutagenicity and genetic instability described *in vivo*.[22,24] Indeed, DNA packaged in an NCP has been shown to be as susceptible to alkylating agents as unpackaged DNA.[25] We have observed in this work that AAG can remove εA lesions from HIGH positions, but has minimal activity on LOW positions. These results suggest that εA repair by AAG at LOW positions *in vivo* may require additional nuclear factors, such as histone variants, histone post-translational modifications, and/or chromatin remodelers to increase access to LOW-positioned lesions.[26,27]

Interestingly, these experiments with global εA lesion NCPs reveal exceptions to the correlation between solution accessibility and AAG activity. Specifically, there are instances of HIGH positions that are inefficiently excised by AAG. The first such position is −74, located near the dyad axis, where only 20% εA excision was observed. The dyad region has been shown to have different characteristics from the rest of the NCP, including less DNA-histone dynamics,[11] a straighter conformation, and being underwound,[9] any of which may contribute to suppressed AAG activity. Consistent with previous studies with restriction enzymes,[10] there is also an overall decrease in DNase I cleavage within the dyad region (Figure S11). Indeed, we[13,16,19] and others[18,28,29] have found that repair of lesions in the ~20 bp of DNA centered at the dyad region is suppressed relative to other regions of the NCP. *In vivo* observations have also shown these patterns of decreased BER within the dyad region of strongly-positioned NCPs.[22]

Sites −30, 96, and 97 are also HIGH positions that are inefficiently excised by AAG, but they are located outside of the inhibitory dyad region. Additionally, all three positions are adjacent to sites where εA is more readily excised. For instance, AAG excised 40% of εA at position −30, but nearly quantitative conversion to product was observed at position −31. These two positions are potentially influenced by the unstructured tails of nearby H2B and/or H2A (Figure S12A). Additionally, these two positions are close to superhelical location (SHL) 5, a location in nucleosomal DNA known for stretching and disrupted base stacking.[14,30] Specifically, the local differences in the dinucleotide step parameters of twist, roll, and slide between the consecutive positions could preferentially prevent AAG excision at position −30. Additionally, DNase I activity in this region was not as robust as in other helical turns on this strand (Figure S11), which might suggest a local NCP structural feature that inhibits general enzymatic activity. Similarly, AAG excised 50% of εA at position 96, while only removing 20% εA at position 97. Reduced εA excision here may be due to the nearby H2B and/or H4 tail (Figure S12B). Alternatively, DNA stretching is also known to occur nearby between SHL ±1 to ±2 to result in severe kinking, and could be a direct result of the very different roll parameters observed between positions 96 and 97,[14,30] and thereby inhibit AAG activity here. It is also of note that both the HRF profile and DNase I activity in this region were high (Figure S11) and could indicate the local NCP architecture is specifically inhibiting AAG activity. Generally across the sequence, the very extreme dinucleotide step parameters of twist, roll, and slide analyzed in 601 NCP structures,[14,30] such as the low degree roll at SHL ± 4.5 (i.e. around positions 28 or 119), or minor groove-

inward pressure point positions, do not appear to influence AAG activity beyond the associated lower-solution accessibility. All other consecutive run εA positions observed, such as 28 and 29; 58 through 60; 89 and 90; −56 and −57; −85 through −88; and −103 and −104, have εA excision correlated with relative solution accessibility as expected. The differential εA excision by AAG in the described positions emphasizes the effects of subtle, local NCP microenvironments unique to each nucleobase position and highlights the complexities that DNA packaging into an NCP presents for a glycosylase. Instances of decreased AAG activity in HIGH positions create an imbalance between damage and repair that can contribute to mutagenic signatures,[23] and describe potential hotspots in the packaged genome for persistent alkylation damage due to a deficiency in repair.

The ends of DNA in NCPs have been shown to spontaneously and transiently unwrap to allow for increased access to nucleobases.[11] Furthermore, NCPs asymmetrically unwrap *in vivo*[31] and *in vitro*,[32,33] meaning that one end is more dynamic than the other. In our global εA NCPs, we observed increased AAG activity at the end known to unwrap preferentially in the 601 NCP.[32,33] From base pair 123 to the DNA end, there is increased repair regardless of solution accessibility (Figure 3). Specifically, at least 60% excision of εA was observed at LOW positions, where similar solution-accessible positions elsewhere in the NCP, like positions 28, 29, −45, 48, 59, −67, −88, had at most 30% excision. MID positions on this end, such as 123, 126, −135, showed at least 80% εA excision, while MID positions on the other end, such as 19, −24, −34, had at most 20%. These results are consistent with *in vivo* observations of higher levels of repair asymmetric to the dyad.[22]

In summary, we determined the repair profile and various kinetic parameters in global DUP and NCPs to observe εA excision by AAG activity at 49 distinct geometric positions. AAG activity across the DUP had maximal amounts of excision, but varying amounts of activity across the NCP architecture. We show that the presence of the histone octamer, and therefore the packaging of DNA into chromatin, modulates repair by AAG. Although AAG's monophasic kinetic behavior remained consistent across the NCP, we observed interesting relationships between the amounts of εA excision and NCP architecture. More specifically, we observed a general correlation between AAG activity and solution accessibility in the NCPs. However, we observed a few exceptions to this correlation, including HIGH positions with low repair likely due to distinct NCP microenvironments that suppress AAG activity, and increased εA removal at the DNA end that asymmetrically unwraps. Our kinetic characterizations of AAG excision of εA in global NCPs have revealed interesting microenvironments that inhibit repair that could not be appreciated previously in site-specific lesion NCPs. Future studies using this global NCP system could provide a more comprehensive understanding of the nuanced relationships between NCP architecture and DNA repair in cells.

MATERIALS AND METHODS

Detailed methods are described in the Supporting Information.

Supplementary Material

Refer to Web version on PubMed Central for supplementary material.

ACKNOWLEDGMENTS

This work was supported by the National Science Foundation (MCB-1817417). EEK was supported by the National Institute of General Medical Sciences (T32GM007601). We thank all members of the Delaney laboratory for discussion and P. Caffrey for critical reading of the manuscript.

REFERENCES

(1). Lindahl T (1993) Instability and decay of the primary structure of DNA. Nature 362, 709–715. [PubMed: 8469282]

(2). Helleday T, Eshtad S, and Nik-Zainal S (2014) Mechanisms underlying mutational signatures in human cancers. Nat. Rev. Genet 15, 585–598. [PubMed: 24981601]

(3). Schermerhorn KM, and Delaney S (2014) A chemical and kinetic perspective on base excision repair of DNA. Acc. Chem. Res 47, 1238–1246. [PubMed: 24646203]

(4). Brooks SC, Adhikary S, Rubinson EH, and Eichman BF (2013) Recent advances in the structural mechanisms of DNA glycosylases. Biochim. Biophys. Acta - Proteins Proteomics 1834, 247–271.

(5). Lee C-YI, Delaney JC, Kartalou M, Lingaraju GM, Maor-Shoshani A, Essigmann JM, and Samson LD (2009) Recognition and processing of a new repertoire of DNA substrates by human 3-methyladenine DNA glycosylase (AAG). Biochemistry 48, 1850–1861. [PubMed: 19219989]

(6). Swenberg JA, Lu K, Moeller BC, Gao L, Upton PB, Nakamura J, and Starr TB (2011) Endogenous versus exogenous DNA adducts: Their role in carcinogenesis, epidemiology, and risk assessment. Toxicol. Sci 120, S130–S145. [PubMed: 21163908]

(7). Segal E, and Widom J (2009) What controls nucleosome positions? Trends Genet 25, 335–343. [PubMed: 19596482]

(8). Richmond RK, Sargent DF, Richmond TJ, Luger K, and Mäder AW (2002) Crystal structure of the nucleosome core particle at 2.8 Å resolution. Nature 389, 251–260.

(9). Hayes JJ, Tullius TD, and Wolffe AP (1990) The structure of DNA in a nucleosome. Proc. Natl. Acad. Sci. U. S. A 87, 7405–7409. [PubMed: 2170977]

(10). Anderson JD, and Widom J (2000) Sequence and position-dependence of the equilibrium accessibility of nucleosomal DNA target sites. J. Mol. Biol 296, 979–987. [PubMed: 10686097]

(11). Kim J, Wei S, Lee J, Yue H, and Lee TH (2016) Single-Molecule Observation Reveals Spontaneous Protein Dynamics in the Nucleosome. J. Phys. Chem. B 120, 8925–8931. [PubMed: 27487198]

(12). Kennedy EE, Caffrey PJ, and Delaney S (2018) Initiating base excision repair in chromatin. DNA Repair (Amst) 71, 87–92. [PubMed: 30170831]

(13). Bilotti K, Tarantino ME, and Delaney S (2018) Human Oxoguanine Glycosylase 1 Removes Solution Accessible 8-Oxo-7,8-dihydroguanine Lesions from Globally Substituted Nucleosomes Except in the Dyad Region. Biochemistry 57, 1436–1439. [PubMed: 29341606]

(14). Vasudevan D, Chua EYD, and Davey CA (2010) Crystal Structures of Nucleosome Core Particles Containing the “601” Strong Positioning Sequence. J. Mol. Biol 403, 1–10. [PubMed: 20800598]

(15). O’Brien PJ, and Ellenberger T (2004) Dissecting the Broad Substrate Specificity of Human 3-Methyladenine-DNA Glycosylase. J. Biol. Chem 279, 9750–9757. [PubMed: 14688248]

(16). Olmon ED, and Delaney S (2017) Differential Ability of Five DNA Glycosylases to Recognize and Repair Damage on Nucleosomal DNA. ACS Chem. Biol 12, 692–701. [PubMed: 28085251]

(17). Bilotti K, Kennedy EE, Li C, and Delaney S (2017) Human OGG1 activity in nucleosomes is facilitated by transient unwrapping of DNA and is influenced by the local histone environment. DNA Repair (Amst) 59, 1–8. [PubMed: 28892740]

(18). Ye Y, Stahley MR, Xu J, Friedman JI, Sun Y, McKnight JN, Gray JJ, Bowman GD, and Stivers JT (2012) Enzymatic excision of uracil residues in nucleosomes depends on the local DNA structure and dynamics. Biochemistry 51, 6028–6038. [PubMed: 22784353]

(19). Li C, and Delaney S (2019) Histone H2A Variants Enhance the Initiation of Base Excision Repair in Nucleosomes. ACS Chem. Biol 14, 1041–1050. [PubMed: 31021597]

(20). Beard BC, Stevenson JJ, Wilson SH, and Smerdon MJ (2005) Base excision repair in nucleosomes lacking histone tails. DNA Repair (Amst) 4, 203–209. [PubMed: 15590328]

(21). Chafin DR, Vitolo JM, Henricksen LA, Bambara RA, and Hayes JJ (2000) Human DNA ligase I efficiently seals nicks in nucleosomes. EMBO J 19, 5492–5501. [PubMed: 11032816]

(22). Mao P, Brown AJ, Malc EP, Mieczkowski PA, Smerdon MJ, Roberts SA, and Wyrick JJ (2017) Genome-wide maps of alkylation damage, repair, and mutagenesis in yeast reveal mechanisms of mutational heterogeneity. Genome Res 27, 1674–1684. [PubMed: 28912372]

(23). Pich O, Muiños F, Sabarinathan R, Reyes-Salazar I, Gonzalez-Perez A, and Lopez-Bigas N (2018) Somatic and Germline Mutation Periodicity Follow the Orientation of the DNA Minor Groove around Nucleosomes. Cell 175, 1074–1087.e18. [PubMed: 30388444]

(24). Levine RL, Yang IY, Hossain M, Pandya GA, Grollman AP, and Moriya M (2000) Mutagenesis induced by a single 1,N6-ethenodeoxyadenosine adduct in human cells. Cancer Res 60, 4098–4104. [PubMed: 10945616]

(25). Trzupek JD, Gottesfeld JM, and Boger DL (2006) Alkylation of duplex DNA in nucleosome core particles by duocarmycin SA and yatakemycin. Nat. Chem. Biol 2, 79–82. [PubMed: 16415862]

(26). Pederson DS, Sweasy JB, Wallace SS, Averill AM, Marsden CG, and Maher RL (2017) Human cells contain a factor that facilitates the DNA glycosylase-mediated excision of oxidized bases from occluded sites in nucleosomes. DNA Repair (Amst) 57, 91–97. [PubMed: 28709015]

(27). Rodriguez Y, Hinz JM, and Smerdon MJ (2015) Accessing DNA damage in chromatin: Preparing the chromatin landscape for base excision repair. DNA Repair (Amst) 32, 113–119. [PubMed: 25957487]

(28). Cole HA, Tabor-Godwin JM, and Hayes JJ (2010) Uracil DNA glycosylase activity on nucleosomal DNA depends on rotational orientation of targets. J. Biol. Chem 285, 2876–2885. [PubMed: 19933279]

(29). Rodriguez Y, and Smerdon MJ (2013) The Structural Location of DNA Lesions in Nucleosome Core Particles Differentially Influence Accessibility of Base Excision Repair Enzymes. J. Biol. Chem 19, 13863–13875.

(30). Chua EYD, Vasudevan D, Davey GE, Wu B, and Davey CA (2012) The mechanics behind DNA sequence-dependent properties of the nucleosome. Nucleic Acids Res 40, 6338–6352. [PubMed: 22453276]

(31). Ramachandran S, Ahmad K, and Henikoff S (2017) Transcription and Remodeling Produce Asymmetrically Unwrapped Nucleosomal Intermediates. Mol. Cell 68, 1038–1053.e4. [PubMed: 29225036]

(32). Ngo TTM, Zhang Q, Zhou R, Yodh JG, and Ha T (2015) Asymmetric unwrapping of nucleosomes under tension directed by DNA local flexibility. Cell 160, 1135–1144. [PubMed: 25768909]

(33). Gansen A, Felekyan S, Kühnemuth R, Lehmann K, Tóth K, Seidel CAM, and Langowski J (2018) High precision FRET studies reveal reversible transitions in nucleosomes between microseconds and minutes. Nat. Commun 9, 4628. [PubMed: 30401903]

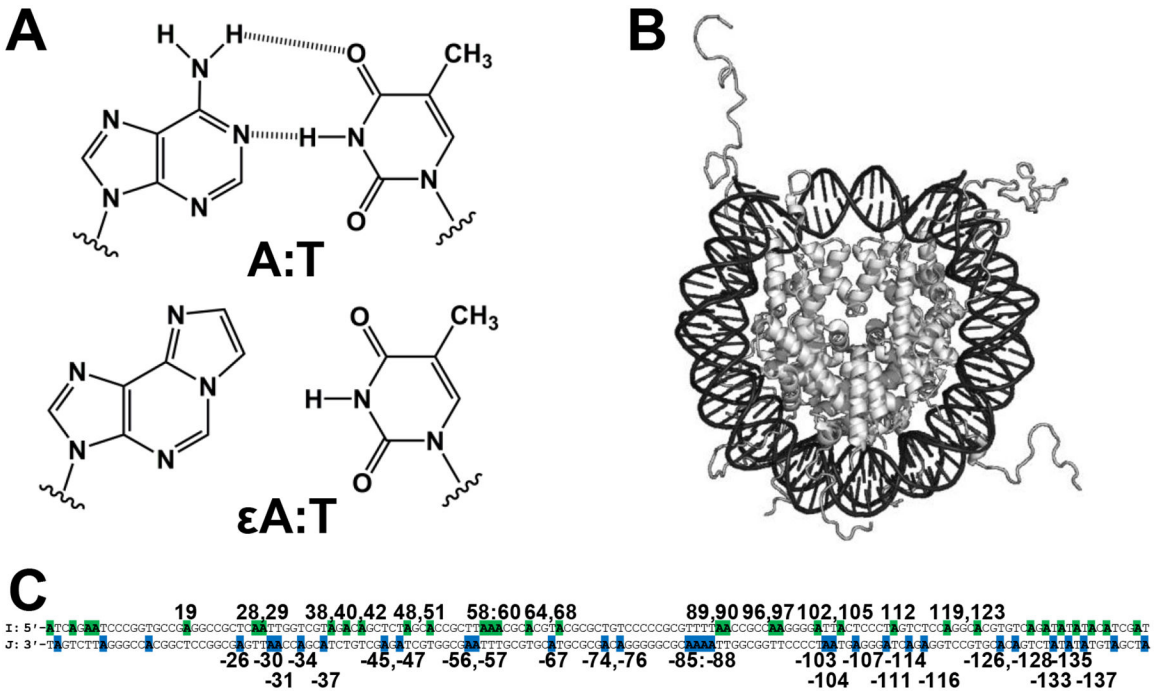

Figure 1.

Representations of lesions, NCP, and DNA sequence. (**A**) An A:T bp and mutagenic εA:T bp. (**B**) Representation of an NCP. (**C**) The 145 bp Widom 601 duplex. Locations of A in sequence are highlighted in the I strand (green) and J strand (blue). Base pairs are numbered starting from the 5′-end of the I strand, with the J strand nucleobase indicated by a negative.

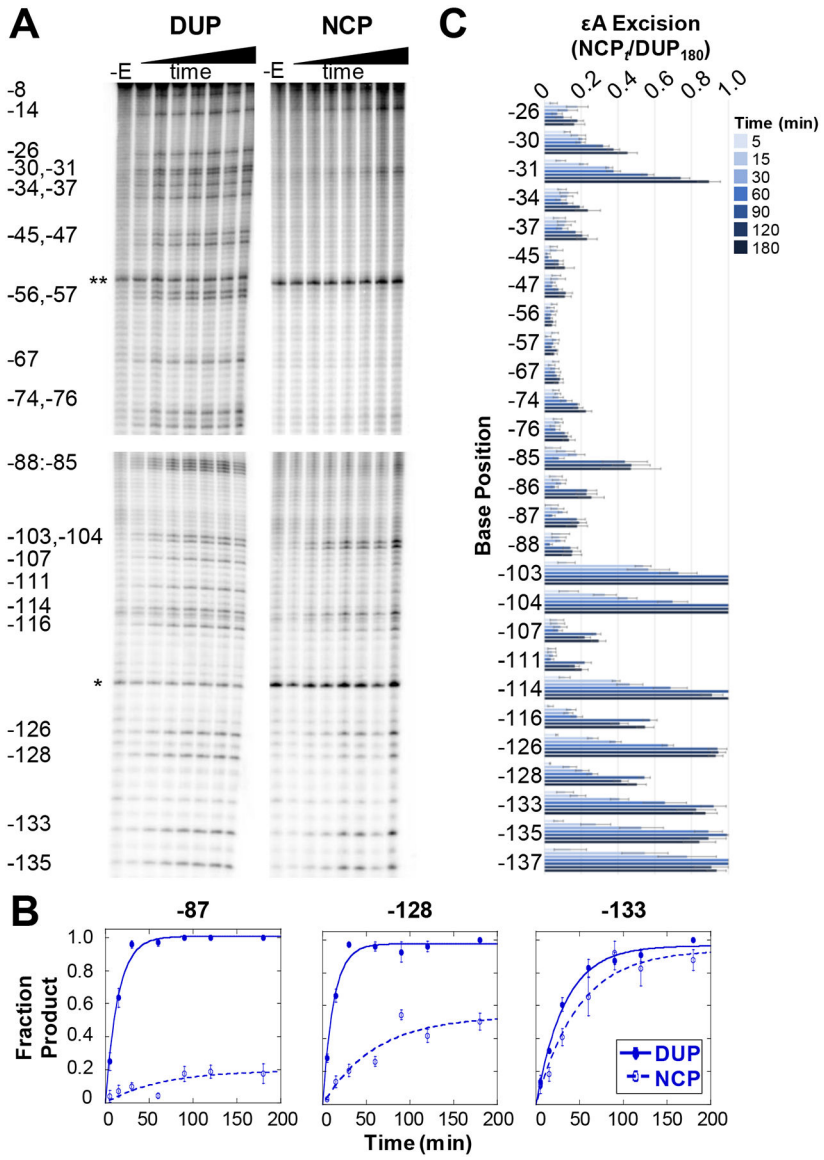

Figure 2.

Single-turnover kinetic time course experiments of εA excision by AAG. (**A**) Representative PAGE gels showing εA excision on the J strand of DUP (left) and NCP (right). DNA samples only treated with NaOH (-E lanes) show incidental damage from experimental conditions and sample workup. Two internal references, a 23 mer (*) and 92 mer (**), used for quantitation are indicated. Four separate gels are shown, indicated by the spaces between the images, with each gel cropped for alignment. The top two panels are aligned to show DUP and NCP data for positions −8 to −76. The bottom two panels are aligned to show data for positions −85 to −135. (**B**) Selected kinetic fits showing examples of low (site −87), medium (site −128), and high (position −133) amounts of εA excision on DUP (closed symbols) and NCPs (open symbols). (**C**) Quantitation of εA excision over time on the J strand in NCPs. Error bars are calculated standard errors (n= 3–10). Analogous data for the I strand in NCPs is shown in Figure S2.

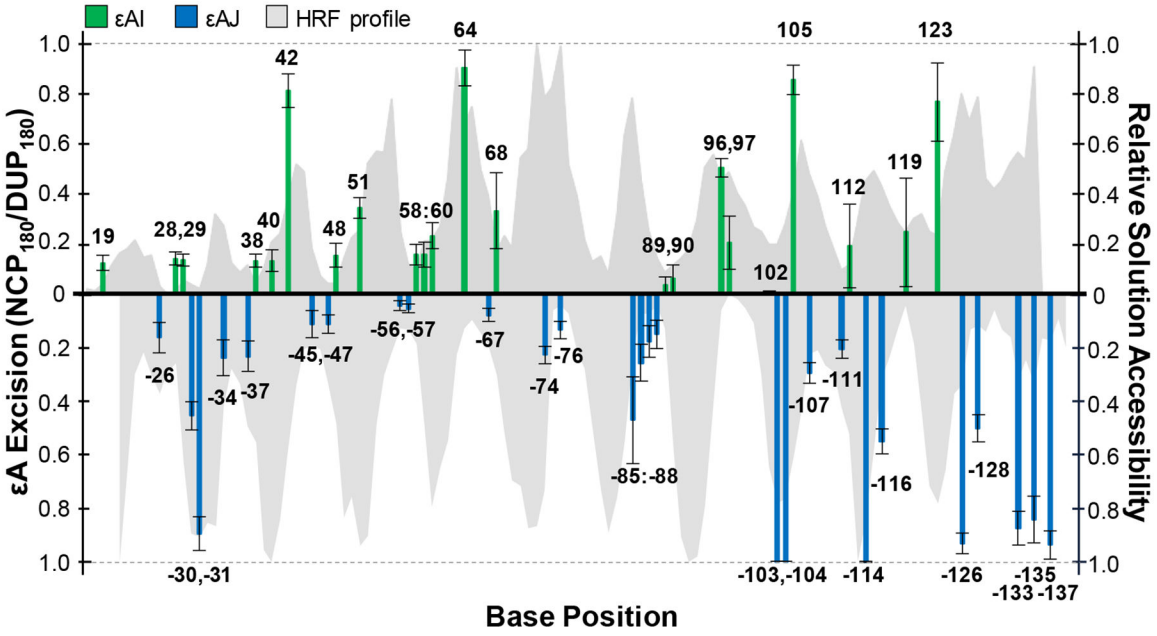

Figure 3.

Relationship between AAG activity on and solution accessibility of εA positions in the NCP. The amount of AAG excision after 180 min is shown as bars at each εA position along the I strand (green) and J strand (blue). Error bars represent the standard error (n = 3–10). The HRF profile characterizes relative reactivity as a function of base position and is depicted as gray area in the background.